Monte Carlo studies of the one-dimensional Ising spin glass with power-law interactions

Helmut G. Katzgraber*
Department of Physics, University of California, Davis, California 95616

A. P. Young†
Department of Physics, University of California, Santa Cruz, California 95064
(Dated: February 11, 2003)

We present results from Monte Carlo simulations of the one-dimensional Ising spin glass with power-law interactions at low temperature, using the parallel tempering Monte Carlo method. For a set of parameters where the long-range part of the interaction is relevant, we find evidence for large-scale droplet-like excitations with an energy that is independent of system size, consistent with replica symmetry breaking. We also perform zero-temperature defect energy calculations for a range of parameters and find a stiffness exponent for domain walls in reasonable, but by no means perfect agreement with analytic predictions.

PACS numbers: 75.50.Lk, 75.40.Mg, 05.50.+q

I. INTRODUCTION

Two main theories of the spin-glass state have been proposed: the "droplet picture"[1–4], and the replica symmetry breaking picture (RSB)[5–8]. The droplet picture states that the minimum energy excitation of linear dimension l containing a given spin (a droplet) has an energy proportional to l^{θ}, where θ is positive (assuming that the transition temperature T_c is finite). It follows that in the thermodynamic limit, excitations that flip a finite fraction of the spins cost an infinite energy. In addition, the droplet picture states that these excitations are fractal with a fractal dimension $d_s < d$, where d is the space dimension. By contrast, RSB follows Parisi's exact solution of the Sherrington-Kirkpatrick (SK) infinite-range model and predicts that excitations involving a finite fraction of the spins cost a finite energy in the thermodynamic limit, and are space filling[9], i.e., $d_s = d$.

There have been several numerical attempts[9–16] to better understand the nature of the spin-glass state for short-range spin glasses. The data, which are on small system sizes, are consistent with a picture in which the "stiffness exponent" for droplet-like excitations is different from that for domain-wall excitations, although it is still unclear if the difference is due to the limited range of system sizes[17], or if it persists in the thermodynamic limit. Recently Krzakala and Martin[10], as well as Palassini and Young[11], find evidence for an intermediate picture (called "TNT" which stands for trivial – non-trivial) in which only a finite amount of energy is needed to generate system-size excitations in the thermodynamic limit, but their surface has a non-trivial fractal dimension less than d.

In addition to finite-T Monte Carlo simulations, there has been a substantial amount of numerical work studying the energy of domain walls at $T = 0$[18–25]. The energy of the domain wall is found to vary as L^{θ} where L is the system size and θ is positive (for systems with $T_c > 0$). The droplet theory assumes that the stiffness exponent for domain walls $\theta_{\mathrm{domain-wall}}$ is the same as the stiffness exponent for droplet-like excitations $\theta_{\mathrm{droplet}}$. In addition, $\theta_{\mathrm{domain-wall}} > 0$. This is in contrast to RSB and TNT where the exponents are expected to be different and $\theta_{\mathrm{droplet}} = 0$. To simplify the notation[26], from now on we will denote $\theta_{\mathrm{domain-wall}}$ by θ and $\theta_{\mathrm{droplet}}$ by θ'.

In this work we consider the question of whether there are one or two stiffness exponents for the case of Ising spin glass models in one-dimension in which the interactions fall off with a power σ of the distance. Depending on σ, the system can have either a finite transition temperature T_c (with the long-range part of the interaction relevant), or $T_c = 0$, in which case it can be either in the short-range or long-range universality class[3,27]. The advantages of this system are (i) a large range of system sizes L can be studied, (ii) there are analytical predictions for the stiffness exponent within the droplet picture, and (iii) within a single model, simply by changing a parameter, one can cover the full range of behavior, from the absence of a spin glass phase to the infinite-range SK model. We perform both Monte Carlo simulations at low-T (which indirectly gives θ'), for a value of σ that has a finite T_c, and ground state calculations for a range of values of σ corresponding to all three regimes: $T_c > 0$, $T_c = 0$ (long-range), and $T_c = 0$ (short-range). We use the parallel tempering[28,29] approach for both the finite-T and $T = 0$ studies.

In Secs. II, III, and IV we introduce the model, observables, and details of the Monte Carlo technique, respectively. In addition we describe the phase diagram of the model in detail. The critical region of the disordered long-range Ising spin glass is analyzed in Sec. V in order to determine the critical temperature of the system and to ensure that in Sec. VI, where we study the system at finite-T, the temperature is sufficiently far below T_c that critical point fluctuations do not affect the data. The zero-temperature results are described in Sec. VII and our conclusions are summarized in Sec. VIII.

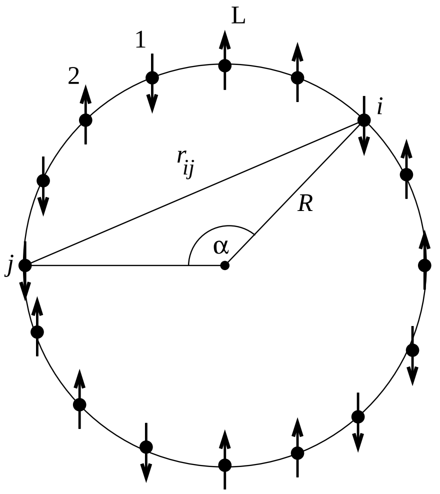

FIG. 1: Geometry of the one-dimensional Ising chain: the Ising spins are placed equidistantly on a ring in order to ensure periodic boundary conditions. Their distance r_{ij} is determined by calculating the geometric distance between the different sites of the circle of radius R and circumference L (not all bonds are shown for clarity).

II. MODEL

The Hamiltonian for the one-dimensional long-range Ising spin glass with power-law interactions is given by

$$\mathcal{H} = -\sum_{i,j} J_{ij} S_i S_j \ , \tag{1}$$

where the sites i lie on a ring of length L, as shown in Fig. 1, and $S_i = \pm 1$ represent Ising spins. We place the spins on a ring in order to ensure periodic boundary conditions. The sum is over all spins on the chain and the couplings J_{ij} are given by

$$J_{ij} = c(\sigma)\frac{\epsilon_{ij}}{r_{ij}^{\sigma}} \ , \tag{2}$$

where the ϵ_{ij} are chosen according to a Gaussian distribution with zero mean and standard deviation unity:

$$\mathcal{P}(\epsilon_{ij}) = \frac{1}{\sqrt{2\pi}} \exp(-\epsilon_{ij}^2/2) \ . \tag{3}$$

The constant $c(\sigma)$ in Eq. (2) is chosen to give a mean-field transition temperature $T_c^{\rm MF} = 1$, where

$$\left(T_c^{\rm MF}\right)^2 = \sum_{j\neq i} [J_{ij}^2]_{\rm av} = c(\sigma)^2 \sum_{j\neq i} \frac{1}{r_{ij}^{2\sigma}} \ . \tag{4}$$

Here $[\cdots]_{\rm av}$ denotes an average over disorder.

The distance between two spins on the chain r_{ij} is determined by $r_{ij} = 2R\sin(\alpha/2)$, where R is the radius of the chain and α is the angle between the two sites on the circle (see Fig. 1). The previous expression can be

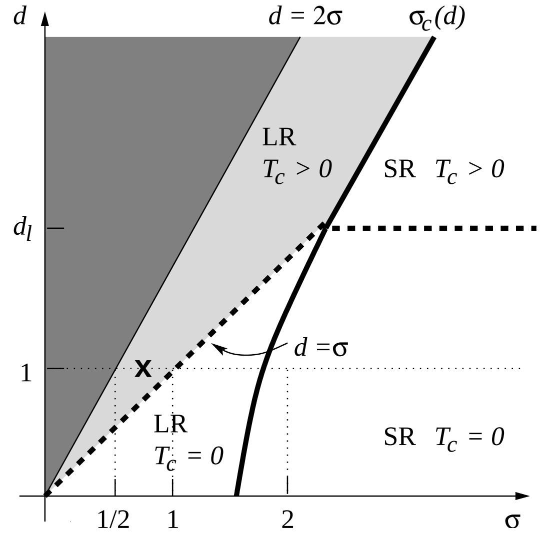

FIG. 2: Sketch of the phase diagram in the d–σ plane for the spin-glass state of the disordered long-range Ising model with power-law interactions following Ref. 3. The light shaded region is where there is both a finite T_c and the spin glass state is controlled by the long-range part of the interaction (i.e. $\theta_{\rm LR} > \theta_{\rm SR}$ and $\theta_{\rm LR} > 0$). The thick solid line separates the region of short-range behavior from that of long-range behavior, i.e. it corresponds to $\theta_{\rm SR} = \theta_{\rm LR}$, and is denoted by $\sigma_c(d)$, see Eq. (7). The thick dashed line separates regions where $T_c = 0$ from regions where $T_c > 0$, i.e. it corresponds to $\theta = 0$, where θ refers to the greater of $\theta_{\rm SR}$ and $\theta_{\rm LR}$. The dark shaded region is where there is no thermodynamic limit unless the interactions are scaled appropriately by system size. The calculations are performed for $d = 1$ (marked by a horizontal dotted line), for which (i) $\sigma_c(d) = 2$, (ii) $\theta > 0$ for $\sigma < 1$, and (iii) the thermodynamic limit does not exist for $\sigma < 1/2$ (unless the interactions are scaled by a power of the system size). These values of sigma are marked. The simulations at finite-T are performed for $\sigma = 3/4, d = 1$, which is indicated by a cross.

rewritten in terms of L and the positions of the spins to obtain

$$r_{ij} = \frac{L}{\pi} \sin\left(\frac{\pi|i-j|}{L}\right) \ . \tag{5}$$

The long-range Ising spin glass with power-law interactions has a very rich phase diagram in the d–σ plane. This is summarized in Fig. 2, which is based on work by Bray *et al.*[27] and by Fisher and Huse[3] who present a detailed analysis of the role of long-range interactions within the droplet model. Spin glass behavior is controlled by the long-range part of the interaction if σ is sufficiently small, and by the short-range part if σ is sufficiently large. More precisely, one has long range behavior if the stiffness exponent of the long-range universality class, $\theta_{\rm LR}$, is greater than that of the short-range universality class, $\theta_{\rm SR}$, and vice-versa. In addition, there is an exact result for $\theta_{\rm LR}$, namely[3,27]

$$\theta_{\rm LR} = d - \sigma, \tag{6}$$

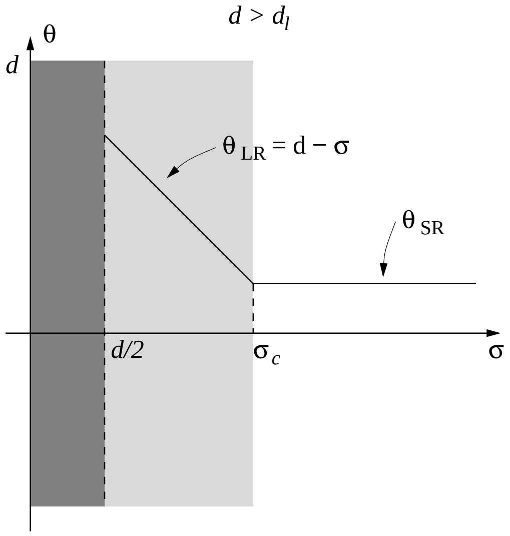

FIG. 3: Stiffness exponent θ as a function of σ for $d > d_l$, where d_l is the lower critical dimension for short-range interactions. The dark shaded region corresponds to $\sigma < d/2$ where T_c diverges unless the interactions are scaled by a power of the system size. The light shaded region is where both $T_c > 0$ and the behavior is governed by the long-range part of the interaction.

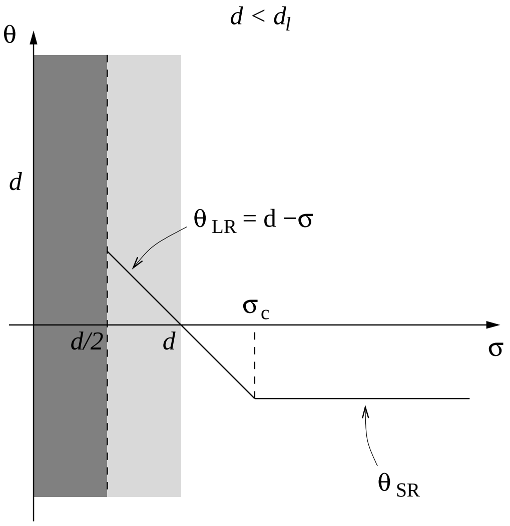

FIG. 4: Same as Fig. 3 but for $d < d_l$.

so long-range behavior occurs if

$$\sigma < \sigma_c(d) = d - \theta_{\rm SR}(d) \ . \tag{7}$$

Equation (6) indicates that critical exponents depend continuously on σ in the long-range region, even though they are independent of σ in the region controlled by the short-range part of the interaction.

The condition for a finite-temperature transition is $\theta > 0$, where θ refers here to the greater of $\theta_{\rm SR}$ and $\theta_{\rm LR}$. For the short range model there is a finite-temperature transition (i.e. $\theta_{\rm SR} > 0$) for d larger than the lower critical dimension d_l, which is found numerically to lie between two and three[18–20,30,31]. In Figs. 3 and 4 we show the expected variation of θ with σ both for $d > d_l$ and $d < d_l$.

For $\sigma < d/2$ the model does not have a thermodynamic limit (T_c diverges) unless the interactions are scaled with an appropriate (inverse) power of L, i.e. $c(\sigma) \to 0$ for $L \to \infty$. Note that $\sigma = 0$ corresponds to the SK model.

For $d = 1$, the case studied in our numerics, one has[18]

$$\theta_{\rm SR}(1) = -1, \tag{8}$$

and so from Eq. (7), $\sigma_c = 2$, in agreement with rigorous results by van Enter and van Hemmen[32]. This situation corresponds to Fig. 4 with $\theta_{\rm SR} = -1$. To obtain a finite-T_c in $d = 1$, one needs $1/2 < \sigma < 1$ and, in the finite-T simulations, we choose $\sigma = 0.75$ (see Fig. 2). For the zero-temperature calculations we use a range of σ between 0.10 and 3.00. From Figs. 2 and 4, we see that this includes all the possible types of behavior: (i) $T_c > 0$, (ii) $T_c = 0$ (LR), (iii) $T_c = 0$ (SR), and (iv) SK-like behavior for $\sigma \to 0$.

III. OBSERVABLES

In our finite-T simulations we primarily focus our attention on the spin overlap defined by

$$q = \frac{1}{L}\sum_{i=1}^{L} S_i^\alpha S_i^\beta , \tag{9}$$

where "α" and "β" refer to two copies (replicas) of the system with the same disorder. In order to determine the critical temperature of the system, we study the Binder ratio[33] g defined by

$$g = \frac{1}{2}\left(3 - \frac{[\langle q^4\rangle]_{\rm av}}{[\langle q^2\rangle]_{\rm av}^2}\right) = \tilde{g}[L^{1/\nu}(T - T_c)] \ . \tag{10}$$

Here, $\langle\cdots\rangle$ represents a thermal average, ν is the correlation length exponent, and T_c the critical temperature of the system. Because g is dimensionless, curves for $g(T, L)$ cross at the same T_c for all L. We also compute the spin-glass susceptibility $\chi_{\rm SG}$, where

$$\chi_{\rm SG} = L[\langle q^2\rangle]_{\rm av} = L^{2-\eta}\tilde{\chi}[L^{1/\nu}(T - T_c)] \ , \tag{11}$$

and η describes the power-law fall-off of the spin-glass correlations at T_c.

IV. EQUILIBRATION

For the finite-T simulations, we use the parallel tempering Monte Carlo method[28,29] as it allows us to study larger systems at lower temperatures than is possible

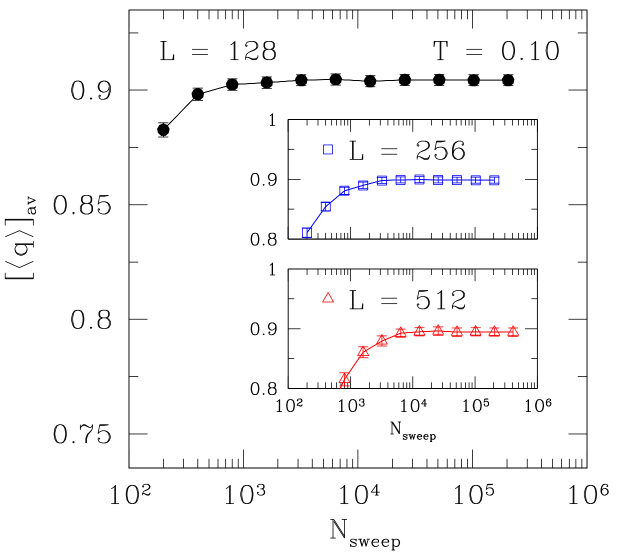

FIG. 5: Average spin overlap $[\langle q \rangle]_{\mathrm{av}}$ as a function of Monte Carlo sweeps N_{sweep}, that each of the replicas perform, averaged over the last half of the sweeps for different system sizes L. Note that the data appear to be independent of the number of sweeps. The data shown is for $T = 0.10$, the lowest temperature studied.

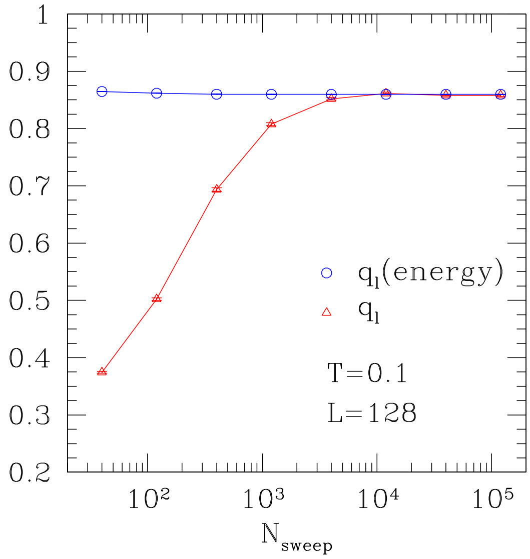

FIG. 6: Test for equilibration using Eq. (13) as discussed in Ref. 12 and the text. The data is for $L = 128, T = 0.1$. The figure shows both the link overlap q_l defined in Eq. (12) and q_l(energy) which is the RHS of Eq. (13), for an increasing number of sweeps N_{sweep} that each replica performs.

with conventional "single spin flip" Monte Carlo methods. We test equilibration by the traditional technique of requiring that different observables are independent of the number of Monte Carlo steps N_{sweep}. Figure 5 shows data for the spin overlap as a function of Monte Carlo steps for different system sizes. We equilibrate by repeatedly doubling the number of Monte Carlo sweeps until the last three agree within error bars.

We also checked the equilibration of some of our data using a generalization of a test that was developed earlier[12] for nearest-neighbor models. For a Gaussian distribution of bonds it is straightforward to show, by integrating by parts with respect to the bonds, that the energy per spin, $U = -N^{-1}\sum_{\langle i,j\rangle}[J_{ij}\langle S_i S_j\rangle]_{\mathrm{av}}$, can be related to a generalized "link overlap" q_l, defined by

$$q_l = \frac{2}{N}\sum_{\langle i,j\rangle}\frac{[J_{ij}^2]_{\mathrm{av}}}{(T_c^{MF})^2}[\langle S_i S_j\rangle^2]_{\mathrm{av}}, \tag{12}$$

as follows:

$$q_l = 1 - \frac{2T|U|}{(T_c^{MF})^2}. \tag{13}$$

Note that this definition of q_l is the natural generalization, to long-range interactions, of the link overlap discussed in earlier work[11,12] on nearest-neighbor models, and that q_l is normalized so that it tends to unity for $T \to 0$ where $\langle S_i S_j\rangle^2 \to 1$.

As discussed in Ref. 12, the two sides of Eq. (13) are only equal to each other in equilibrium and approach the equilibrium value from opposite sides. This is illustrated in Fig. 6 which shows q_l and the quantity on the RHS of Eq. (13) for an increasing number of sweeps for $L = 128, T = 0.1$. The two quantities do indeed approach each other from opposite sides, and once they agree they do not change if the simulation is run for longer. We applied this test for several lattice sizes using the parameters in Table I, and found that the data was well equilibrated in each case.

We also require that the acceptance ratios for the global moves which interchange the different temperatures in the parallel tempering scheme be greater than 0.4 on average and roughly constant as a function of temperature. Table I shows the number of samples N_{samp} and the number of Monte Carlo sweeps N_{sweep} performed by each replica for each lattice size. The lowest temperature used is $T = 0.10$, the highest $T = 1.40$, well above the mean-field critical temperature $T_c^{\mathrm{MF}} = 1$.

We also use parallel tempering as an optimization algorithm to determine the ground state in the $T = 0$ calculations. This is described in Sec. VII.

V. FINITE-SIZE SCALING IN THE CRITICAL REGION

In this section we determine the critical temperature T_c and the critical exponents for the disordered chain with $\sigma = 0.75$. In Fig. 7 we show rescaled data for the

TABLE I: Parameters of the finite-T simulations. $N_{\rm samp}$ is the number of samples, i.e., sets of disorder realizations, $N_{\rm sweep}$ is the total number of sweeps simulated for each of the $2N_T$ replicas for a single sample, and N_T is the number of temperatures used in the parallel tempering method.

L	$N_{\rm samp}$	$N_{\rm sweep}$	N_T
32	2.0×10^4	1.0×10^4	23
64	2.0×10^4	1.0×10^4	23
128	2.0×10^4	2.0×10^4	23
256	1.0×10^4	1.0×10^5	23
512	5.0×10^3	2.0×10^5	23

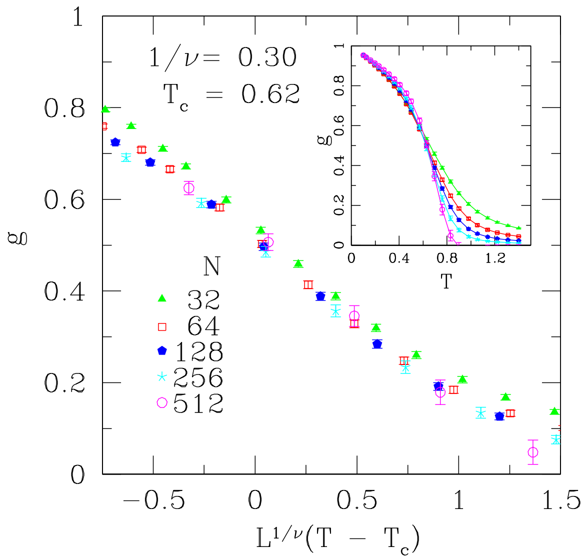

FIG. 7: The Binder ratio g as a function of $L^{1/\nu}(T-T_c)$ for several system sizes. We see that the data scale well for $1/\nu = 0.30 \pm 0.03$ and $T_c = 0.62 \pm 0.03$. This is a little lower than the (approximate) estimate of Bhatt and Young[35] who find $T_c \approx 0.68$. The inset shows the unscaled data for g. One can see that the data for different sizes cross at $T \sim 0.62$.

Binder ratio g as a function of temperature for different system sizes [see Eq. (10)]. The data scale well for $T_c = 0.62 \pm 0.03$ and $1/\nu = 0.30 \pm 0.03$, and agree with previous results by Leuzzi[34]. The inset of the aforementioned figure shows the unscaled data for g which cross at $T_c \approx 0.62$. The error bars are estimated by varying g slightly until the data do not collapse well.

We use the same approach below for the spin-glass susceptibility, for which the data, rescaled according to Eq. (11), is presented in Fig. 8. The data scale well for $\eta = 1.34 \pm 0.03$ and the previously mentioned values of $1/\nu$ and T_c. These values can be compared with the results of Kotliar *et al.*[36]: $\eta = 3 - 2\sigma$ $(= 1.5)$, and $1/\nu = (1/3) - 4\epsilon$ to first order in ϵ, where $\epsilon = \sigma - 2/3$. The latter gives $1/\nu = 0$ suggesting that truncating the expansion to first order in ϵ is not valid for $\sigma = 3/4$.

Having studied the critical region of the model to estimate T_c we are now able to simulate the system at low

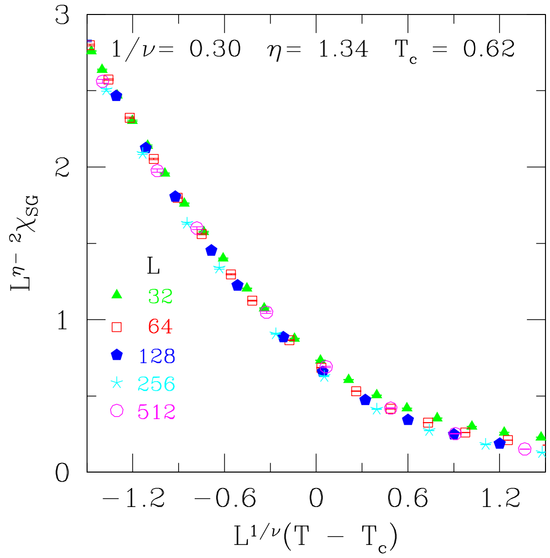

FIG. 8: Data for the rescaled spin-glass susceptibility $L^{\eta-2}\chi_{\rm SG}$ for different sizes as a function of $L^{1/\nu}(T-T_c)$. The data scale well for $1/\nu = 0.30 \pm 0.03$, $T_c = 0.62 \pm 0.03$, and $\eta = 1.34 \pm 0.03$.

temperatures ($T \approx 0.16 T_c$) in order to probe the spin-glass phase and test if $\theta = \theta'$.

VI. RESULTS AT LOW TEMPERATURES

In this section we study the model with $\sigma = 0.75, d = 1$, marked by "x" in Fig. 2, at temperatures well below $T_c \simeq 0.62$, in order to get information about large-scale, low-energy excitations in the spin-glass state.

Differences between the various models for the spin glass state can be quantified by studying[9,12,37–39] $P(q)$, the distribution of the spin-glass overlap q. RSB predicts a nontrivial distribution with a finite weight in the tail down to $q = 0$, independent of system size. On the contrary, the droplet picture predicts that $P(q)$ should be trivial with only two peaks at $\pm q_{\rm EA}$, where $q_{\rm EA}$ is the Edwards-Anderson order parameter. For finite systems there is also a tail down to $q = 0$ but this vanishes in the thermodynamic limit like[1,4,40] $\sim L^{-\theta'}$ with $\theta' = \theta$.

Figures 9 and 10 show data for $P(q)$ at temperatures 0.10 and 0.23, respectively. There is clearly a peak for large q and a tail down to $q = 0$. At both temperatures one sees that the tail in the distribution is essentially independent of system size. A more precise determination of the size dependence of $P(0)$ is shown in Fig. 11 where, to improve statistics, we average over the q-values with $|q| < q_\circ$, with $q_\circ = 0.50$. The expected[1,4,40] behavior in the droplet model is $P(0) \sim L^{-\theta'}$, with $\theta' = \theta$ where[3,27] $\theta = d - \sigma$. The dashed line in Fig. 11 has slope -0.25, the expected value for $\sigma = 0.75$ according to the droplet model. The size dependence is consistent with a constant

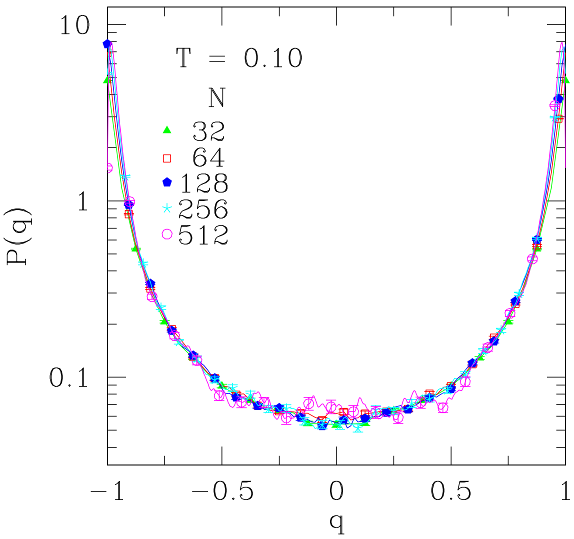

FIG. 9: Data for the overlap distribution $P(q)$ at $T = 0.10$. Note that the vertical scale is logarithmic to better make visible both the peak at large q and the tail down to $q = 0$. In this, as well as in Fig. 10, we only display *some* of the data points as symbols, for clarity, but the lines connect *all* the data points. This accounts for the curvature in some of the lines between neighboring symbols. In this paper all distributions are normalized so that the area shown under the curve is unity.

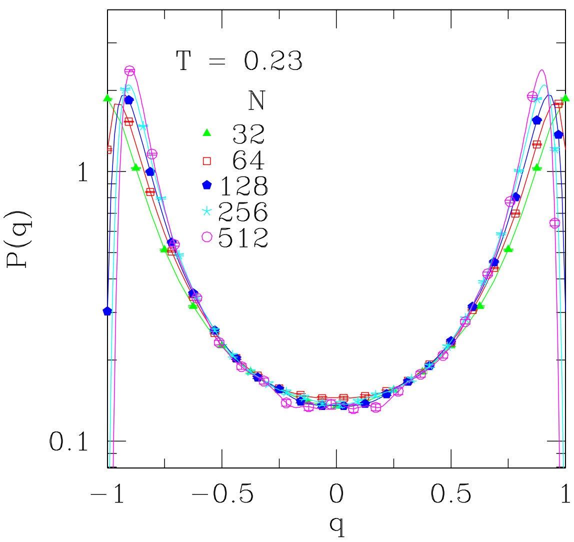

FIG. 10: Same as for Fig. 9 but at $T = 0.23$.

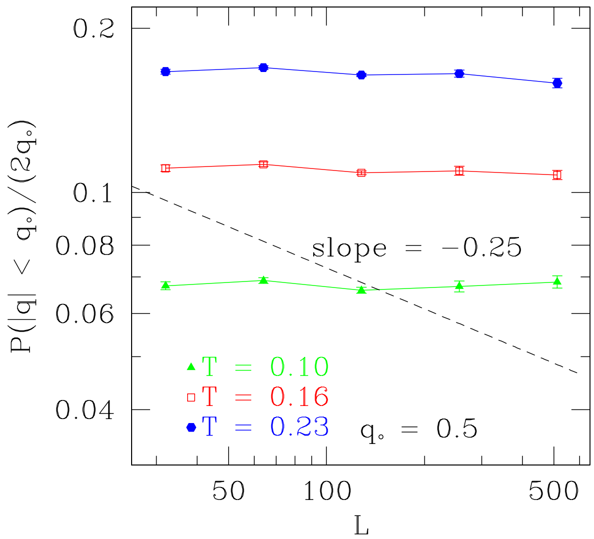

FIG. 11: Log-log plot of $P(|q| < q_\circ)/(2q_\circ)$, the spin overlap distribution for small q, against L for $q_\circ = 0.50$. The data is observed to not depend significantly on the system size L. The dashed line has slope -0.25, the theoretical prediction of the droplet model[3]. Asymptotically, the data should be parallel to this line according to the droplet theory.

$P(0)$, which implies that the energy to create a large excitation does not increase with size, at least for the range of sizes studied here.

We perform a two-parameter fit of the data in Fig. 11 of the form $aL^{-\theta'}$ to find for $T = 0.10$, $\theta' = -0.005 \pm 0.009$, for $T = 0.16$, $\theta' = -0.020 \pm 0.007$, and for $T = 0.23$, $\theta' = -0.016 \pm 0.006$. The fitting probabilities[41] Q for the different temperatures are 0.135, 0.186, and 0.08, respectively, which is reasonable. Fixing $\theta' = 0$ we obtain fitting probabilities of 0.214, 0.053, and 0.076, respectively. On the contrary, fixing $\theta' = 0.25$, the predicted value for the droplet picture, we find $Q \lesssim 10^{-31}$ for all three temperatures. Hence we are confident that, within error bars, $\theta' \simeq 0$ for the range of sizes studied.

Moore[42] has argued that $P(q)$ should be trivial in the thermodynamic limit (i.e. just two delta functions at $q = \pm q_{EA}$) to first order in an expansion about the "lower critical dimension" $\sigma = 1$. This seems to disagree with our numerics, although possibly even larger sizes might be necessary to see the asymptotic behavior.

VII. DOMAIN WALL ENERGIES AT ZERO TEMPERATURE

Since there are analytic predictions, Eqs. (6) and (8), for θ for the present model, it is useful to directly calculate θ from zero-temperature domain-wall calculations for different values of σ.

We use parallel tempering here as an optimization algorithm. We find that if we take the lowest temperature, $T_{\min}$, to be 0.05, then the minimum energy state found at this temperature is the ground state. To test whether the true ground state has been reached two criteria were adopted: (i) the same minimum energy state has to be reached from two replicas at $T_{\min}$ for all samples, and (ii) this state has to be reached during the first 1/4 of the

TABLE II: Parameters of the $T = 0$ simulations. The table shows the total number of Monte Carlo steps used for each value of σ and L.

σ	$L = 16$	$L = 32$	$L = 64$	$L = 128$	$L = 256$
0.10	2×10^3	4×10^3	8×10^3	4×10^4	12×10^4
0.25	2×10^3	4×10^3	8×10^3	4×10^4	12×10^4
0.50	2×10^3	4×10^3	8×10^3	4×10^4	12×10^4
0.62	2×10^3	4×10^3	8×10^3	4×10^4	12×10^4
0.75	2×10^3	4×10^3	8×10^3	4×10^4	12×10^4
0.87	2×10^3	4×10^3	8×10^3	4×10^4	12×10^4
1.00	2×10^3	4×10^3	8×10^3	8×10^4	6×10^5
1.25	2×10^3	4×10^3	6×10^4	6×10^5	—
1.50	2×10^3	4×10^3	6×10^4	—	—
1.75	2×10^3	4×10^3	6×10^4	—	—
2.00	2×10^3	4×10^3	6×10^4	—	—
2.50	2×10^3	4×10^3	2×10^5	—	—
3.00	2×10^3	4×10^3	2×10^5	—	—

sweeps in both copies. These conditions were satisfied for the parameters used in the simulations which are shown in Table II.

Having found the ground state with periodic (P) boundary conditions, we then flip the boundary conditions to "anti-periodic" (AP) by the following prescription. Consider one of the nearest neighbor (nn) bonds, e.g. that between sites 1 and L in Fig. 1. Then, for all i and j, change the sign of the bond between i and j if the shorter path between those sites goes through the chosen nn bond. The new ground state is calculated and note is taken of the difference in energy

$$\delta E = E_{\mathrm{AP}} - E_{\mathrm{P}} \tag{14}$$

for each sample. On average, there is no preference for AP or P and so $[\delta E]_{\mathrm{av}} = 0$. Hence we take the average of the absolute value

$$\Delta E = [\,|\delta E|\,]_{\mathrm{av}} \tag{15}$$

as a measure of the characteristic domain wall energy.

Data for a range of sizes and values of σ is shown in Fig. 12. Our program automatically scales the interactions to set $T_c^{MF} = 1$, so no modifications are needed for the case $\sigma \le 0.5$ since the fact that the scale factor $c(\sigma)$ (in Eqs. (2) and (4)) tends to zero for $L \to \infty$ in this range, is taken care of automatically.

A smaller range of sizes has been studied for larger σ as parallel tempering is less efficient in finding the ground state in this limit. At first sight this seems surprising because the nearest-neighbor interactions dominate and so there is no frustration, apart possibly from that due to the boundary conditions. The spins become stuck when a frustrated nn bond is larger in magnitude than the neighboring bonds. Parallel tempering does not seem to help much in this situation, perhaps because the local minima do not have a hierarchical structure. It would be interesting to investigate in more detail the conditions under which parallel tempering is efficient.

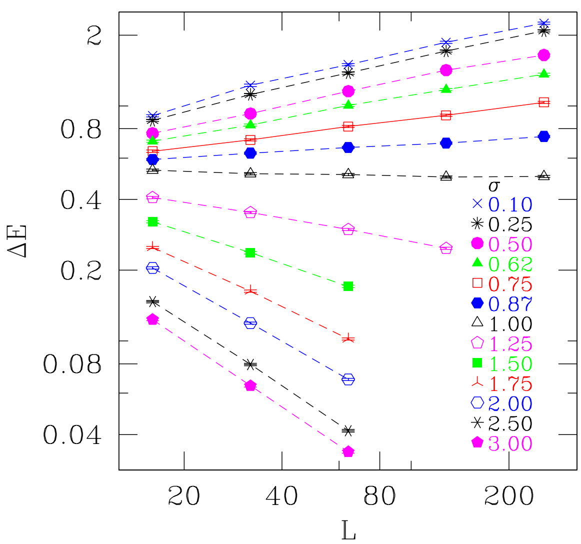

FIG. 12: Data for the defect energy $\Delta E = [\,|E_{\mathrm{P}} - E_{\mathrm{AP}}|\,]_{\mathrm{av}}$ for different sizes and values of σ. The solid lines connects the data for $\sigma = 0.75$, the value of σ studied at finite temperatures.

TABLE III: Fits for $\Delta E \sim aL^{\theta}$ for different values of σ. Q represents the quality of fit. The last column in the table shows the range of values of L used in the fits (for the possible values see Table II). For $0.10 \le \sigma \le 0.25$ we exclude the data for $L = 16$ from the fits due to finite-size effects for small values of σ.

σ	a	θ	Q	L-Range
0.10	-0.818 ± 0.033	0.295 ± 0.007	0.495	32 – 256
0.25	-0.928 ± 0.032	0.301 ± 0.007	0.759	32 – 256
0.50	-1.023 ± 0.033	0.282 ± 0.005	0.007	16 – 256
0.62	-1.007 ± 0.022	0.239 ± 0.005	0.235	16 – 256
0.75	-0.925 ± 0.022	0.173 ± 0.005	0.852	16 – 256
0.87	-0.741 ± 0.021	0.079 ± 0.005	0.801	16 – 256
1.00	-0.577 ± 0.022	-0.023 ± 0.005	0.319	16 – 256
1.25	-0.225 ± 0.028	-0.239 ± 0.007	0.222	16 – 128
1.50	0.137 ± 0.030	-0.457 ± 0.011	0.349	16 – 64
1.75	0.414 ± 0.041	-0.647 ± 0.012	0.150	16 – 64
2.00	0.600 ± 0.042	-0.788 ± 0.012	0.727	16 – 64
2.50	0.619 ± 0.044	-0.913 ± 0.013	0.289	16 – 64
3.00	0.499 ± 0.045	-0.935 ± 0.013	0.975	16 – 64

One expects that $\Delta E \sim L^{\theta}$, where $\theta = 1 - \sigma$ in the long-range region $1/2 < \sigma < 2$, and $\theta = -1$ in the short-range region $\sigma > 2$. Fits to the data obtained in Fig. 12, along with the analytic prediction, are shown in Fig. 13 and in Table III. In particular, there is a distinctive positive slope for $\sigma = 0.75$ in Fig. 12 (solid line), corresponding to a positive value of θ. This is in clear contrast to the finite-T data shown in Fig. 11.

We see that the overall trends in the analytic prediction are reproduced by the data, but there is some rounding where the analytical result has a change in slope. Note that our results for θ always lie well below $1/2$, the

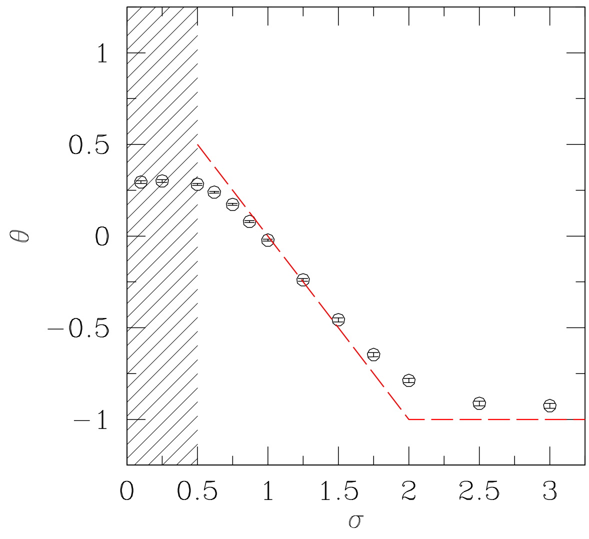

FIG. 13: Variation of θ, with σ, obtained from fitting the data in Fig. 12 to $\Delta E \sim L^{\theta}$. Also shown is the analytic prediction (dashed line): $\theta = 1 - \sigma$ for $1/2 < \sigma < 2$, and $\theta = -1$ for $\sigma > 2$. The shaded region is where there is no thermodynamic limit unless the interactions are scaled appropriately by system size.

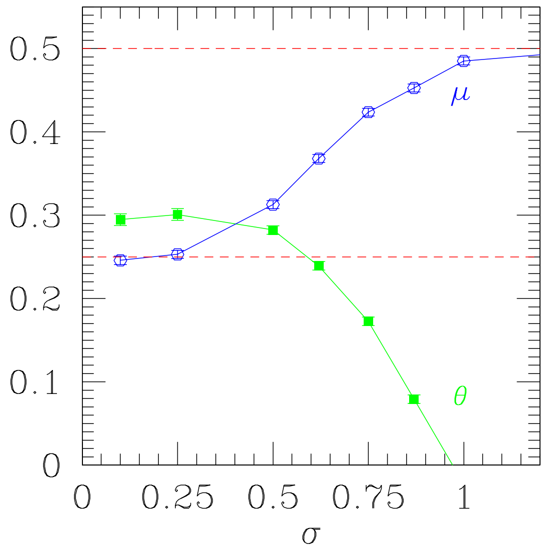

FIG. 14: Defect energy exponent θ and the exponent for the rms sample-to-sample fluctuations in the ground state energy, μ, for different values of σ.

predicted[3,27] value for $\sigma = 1/2$, and appears to saturate at about 0.3 as $\sigma \to 0$, the SK limit.

In recent work Aspelmeier *et al.*[43] have given analytic arguments, based on RSB theory, that the defect energy should vary as N^{μ} for short range models in high dimension d, where $N = L^d$ and μ is the exponent for the rms sample-to-sample fluctuations of the free energy of the SK model. A number of authors[44–46] have found that $\mu \simeq 1/4$, at least at $T = 0$. We have therefore calculated μ for our one-dimensional model at $T = 0$ for different values of σ and show the results in Fig. 14. Indeed we find that $\mu \simeq 1/4$ for $\sigma \to 0$ (the SK limit). Also note that it crosses over to the expected "self-averaging" value of $\mu = 1/2$ in the region $\sigma > 1/2$ where we no longer need to scale the interactions with system size. Since we work in $d = 1$ the expectation from Aspelmeier *et al.*[43] is that $\theta \to \mu$ for $\sigma \to 0$. Fig. 14 also shows θ and, indeed, it is quite striking how θ becomes close to μ at small σ.

VIII. CONCLUSIONS

We have performed finite-T Monte Carlo simulations and ground state calculations of the long-range disordered Ising chain in one dimension with power-law interactions. For the ground-state calculations we have studied a range of values of σ that encompasses all the possible regimes, from large σ where the system is controlled by the short-range part of the interactions and has $T_c = 0$, all the way to near the SK model limit, $\sigma = 0$. For the finite-temperature Monte Carlo runs we have concentrated on a single value of σ, namely 0.75, which is in the range where there is a finite T_c.

For $\sigma = 0.75$ we find the stiffness exponent for droplets, θ', inferred from Monte Carlo simulations for sizes up to $L = 512$, to be close to zero, whereas the stiffness exponent for domain walls, θ, is positive. We find $\theta = 0.173 \pm 0.005$ (only statistical errors included) somewhat lower than the analytic prediction[3,27] that $\theta = 0.25$. These results are consistent with the RSB and TNT scenarios according to which $\theta' = 0$ and $\theta \neq \theta'$. Similar results have been found in earlier work on short range models in three and four dimensions[10–12]. According to the droplet picture, $\theta' = \theta$ asymptotically, and there has been discussion as to whether the failure of the numerics to see this is an artifact of the small lattice sizes[17], or whether it will persist in the thermodynamic limit. In the present work, the disagreement persists even though we are able to study a much larger range of L.

Also noteworthy is our finding that θ tends to a value of about 0.3 for $\sigma \to 0$, the SK model limit. This is below the droplet theory prediction that θ should tend to $1/2$ for $\sigma \to 0$, but is close to the prediction of Aspelmeier et al.[43] that $\theta \to 1/4$ in this limit.

Acknowledgments

We would like to that M. A. Moore for stimulating discussions and for bringing Ref. 42 to our attention, and G. Blatter for carefully reading the manuscript. HGK acknowledges support from the National Science Foundation under grant No. DMR 9985978 and the Swiss National Science Foundation. APY acknowledges support from the National Science Foundation under grant No. DMR 0086287, and the EPSRC under grant GR/R37869/01. He would also like to thank David Sherrington for hospitality during his stay at Oxford. This research was supported in part by NSF cooperative agreement ACI-9619020 through computing resources provided by the National Partnership for Advanced Computational Infrastructure at the San Diego Supercomputer Center. We would like to thank the University of New Mexico for access to their Albuquerque High Performance Computing Center. This work utilized the UNM-Alliance Los Lobos Supercluster. Part of the simulations were performed on the Asgard cluster at ETH Zürich.

---

[*] Current address: Theoretische Physik, ETH Hönggerberg, CH-8093 Zürich, Switzerland

[†] Electronic address: `peter@bartok.ucsc.edu`; URL: `http://bartok.ucsc.edu/peter`

[1] D. S. Fisher and D. A. Huse, *Ordered phase of short-range Ising spin-glasses*, Phys. Rev. Lett. **56**, 1601 (1986).

[2] D. S. Fisher and D. A. Huse, *Absence of many states in realistic spin glasses*, J. Phys. A **20**, L1005 (1987).

[3] D. S. Fisher and D. A. Huse, *Equilibrium behavior of the spin-glass ordered phase*, Phys. Rev. B **38**, 386 (1988).

[4] A. J. Bray and M. A. Moore, *Scaling theory of the ordered phase of spin glasses*, in *Heidelberg Colloquium on Glassy Dynamics and Optimization*, edited by L. Van Hemmen and I. Morgenstern (Springer, New York, 1986), p. 121.

[5] G. Parisi, *Infinite number of order parameters for spin-glasses*, Phys. Rev. Lett. **43**, 1754 (1979).

[6] G. Parisi, *The order parameter for spin glasses: a function on the interval* 0–1, J. Phys. A. **13**, 1101 (1980).

[7] G. Parisi, *Order parameter for spin-glasses*, Phys. Rev. Lett. **50**, 1946 (1983).

[8] M. Mézard, G. Parisi, and M. A. Virasoro, *Spin Glass Theory and Beyond* (World Scientific, Singapore, 1987).

[9] E. Marinari and G. Parisi, *On the effects of changing the boundary conditions on the ground state of Ising spin glasses*, Phys. Rev. B **62**, 11677 (2000).

[10] F. Krzakala and O. C. Martin, *Spin and link overlaps in 3-dimensional spin glasses*, Phys. Rev. Lett. **85**, 3013 (2000), (cond-mat/0002055).

[11] M. Palassini and A. P. Young, *Nature of the spin glass state*, Phys. Rev. Lett. **85**, 3017 (2000), (cond-mat/0002134).

[12] H. G. Katzgraber, M. Palassini, and A. P. Young, *Monte Carlo simulations of spin glasses at low temperatures*, Phys. Rev. B **63**, 184422 (2001), (cond-mat/0007113).

[13] H. G. Katzgraber and A. P. Young, *Nature of the spin-glass state in the three-dimensional gauge glass*, Phys. Rev. B **64**, 104426 (2001), (cond-mat/0105077).

[14] H. G. Katzgraber and A. P. Young, *Monte Carlo simulations of the four dimensional XY spin-glass at low temperatures*, Phys. Rev. B **65**, 214401 (2002), (cond-mat/0108320).

[15] J. Houdayer, F. Krzakala, and O. C. Martin, *Large-scale low-energy excitations in 3-d spin glasses*, Eur. Phys. J. B. **18**, 467 (2000).

[16] J. Houdayer and O. C. Martin, *A geometric picture for finite dimensional spin glasses*, Europhys. Lett. **49**, 794 (2000).

[17] M. A. Moore, *Corrections to scaling in the droplet picture of spin glasses* (2002), (cond-mat/0203469).

[18] A. J. Bray and M. A. Moore, *Lower critical dimension of Ising spin glasses: a numerical study*, J. Phys. C **17**, L463 (1984).

[19] W. L. McMillan, *Domain-wall renormalization-group study of the three-dimensional random Ising model*, Phys. Rev. B **30**, 476 (1984).

[20] W. L. McMillan, *Domain-wall renormalization-group study of the two-dimensional random Ising model*, Phys. Rev. B **29**, 4026 (1984).

[21] H. Rieger, L. Santen, U. Blasum, M. Diehl, M. Jünger, and G. Rinaldi, *The critical exponents of the two-dimensional Ising spin glass revisited: exact ground-state calculations and Monte Carlo simulations*, J. Phys. A **29**, 3939 (1996).

[22] A. K. Hartmann, *Scaling of stiffness energy for three-dimensional* $\pm J$ *Ising spin glasses*, Phys. Rev. E **59**, 84 (1999).

[23] M. Palassini and A. P. Young, *Triviality of the ground state structure in Ising spin glasses*, Phys. Rev. Lett. **83**, 5126 (1999), (cond-mat/9906323).

[24] A. K. Hartmann and A. P. Young, *Lower critical dimension of Ising spin glasses*, Phys. Rev. B **64**, 180404 (2001), (cond-mat/0107308).

[25] A. C. Carter, A. J. Bray, and M. A. Moore, *Aspect-ratio scaling and the stiffness exponent* θ *for Ising spin glasses*, Phys. Rev. Lett. **88**, 077201 (2002), (cond-mat/0108050).

[26] Houdayer and Martin[16] introduce *three* exponents: θ_{dw} for domain-wall excitations, θ_g for low-energy system-size excitations, and θ_l for droplets of size $l \ll L$, where L is the size of the system studied. The exponent θ introduced here corresponds to θ_{dw} from Ref. 16, whereas θ' corresponds to θ_g. Note that in this work we do *not* calculate θ_l.

[27] A. J. Bray, M. A. Moore, and A. P. Young, *Lower critical dimension of metallic vector spin-glasses*, Phys. Rev. Lett **56**, 2641 (1986).

[28] K. Hukushima and K. Nemoto, *Exchange Monte Carlo method and application to spin glass simulations*, J. Phys. Soc. Japan **65**, 1604 (1996).

[29] E. Marinari, *Optimized Monte Carlo methods*, in *Advances in Computer Simulation*, edited by J. Kertész and I. Kondor (Springer Verlag, Berlin, 1998), p. 50, (cond-mat/9612010).

[30] N. Kawashima and A. P. Young, *Phase transition in the three-dimensional* $\pm J$ *Ising spin glass*, Phys. Rev. B **53**, R484 (1996).

[31] H. G. Ballesteros, A. Cruz, L. Fernandez, V. Martin-Mayor, J. Pech, J. J. Ruiz-Lorenzo, A. Tarancon, P. Tellez, C. L. Ullod, and C. Ungil, *Critical behavior of the three-dimensional Ising spin glass*, Phys. Rev. B **62**, 14237 (2000), (cond-mat/0006211).

[32] A. C. D. van Enter and J. L. van Hemmen, *The thermodynamic limit for long-range random systems*, J. Stat. Phys. **39**, 1 (1985).

[33] K. Binder, *Critical properties from Monte Carlo coarse graining and renormalization*, Phys. Rev. Lett. **47**, 693 (1981).

[34] L. Leuzzi, *Critical behaviour and ultrametricity of ising spin-glass with long-range interactions*, J. Phys. A **32**, 1417 (1999).

[35] R. N. Bhatt and A. P. Young, *Long range Ising spin glasses: Critical behavior and ultrametricity*, J. Magn. and Magn. Mat. **54-57**, 191 (1986).

[36] G. Kotliar, P. W. Anderson, and D. L. Stein, *One-dimensional spin-glass model with long-range random interactions*, Phys. Rev. B **27**, 602 (1983).

[37] J. D. Reger, R. N. Bhatt, and A. P. Young, *A Monte Carlo study of the order parameter distribution in the four-dimensional Ising spin glass*, Phys. Rev. Lett. **64**, 1859 (1990).

[38] E. Marinari, G. Parisi, and J. J. Ruiz-Lorenzo, *Numerical simulations of spin glass systems*, in *Spin Glasses and Random Fields*, edited by A. P. Young (World Scientific, Singapore, 1998), p. 59.

[39] E. Marinari and F. Zuliani, *Numerical simulations of the 4d Edwards-Anderson spin glass with binary couplings*, J. Phys. A **32**, 7447 (1999).

[40] M. A. Moore, H. Bokil, and B. Drossel, *Evidence for the droplet picture of spin glasses*, Phys. Rev. Lett. **81**, 4252 (1998).

[41] W. H. Press, S. A. Teukolsky, W. T. Vetterling, and B. P. Flannery, *Numerical Recipes in C* (Cambridge University Press, Cambridge, 1995).

[42] M. A. Moore, *One-dimensional Ising spin-glass model with long range interactions*, J. Phys. A **19**, L211 (1986).

[43] T. Aspelmeier, M. A. Moore, and A. P. Young, *Interface energies in Ising spin glasses* (2002), (cond-mat/0006211).

[44] S. Cabasino, E. Marinari, P. Paolucci, and G. Parisi, *Eigenstates and limit cycles in the SK model*, J. Phys. A. **21**, 4201 (1988).

[45] J.-P. Bouchaud, F. Krzakala, and O. Martin, *Energy exponents and corrections to scaling in Ising spin glasses*, (cond-mat/0108050) (2002).

[46] M. Palassini (2003), (manuscript in preparation.).